Available online at www.sciencedirect.com
SCIENCE DIRECT
Journal of Magnetic Resonance 180 (2006) 186–196
JMR Journal of Magnetic Resonance
www.elsevier.com/locate/jmr

Effective dipolar couplings determined by dipolar dephasing of double-quantum coherences

Jörn Schmedt auf der Günne *

Munich University (LMU), Department of Chemistry and Biochemistry, Butenandtstr. 5-13 (house D), 81377 Munich, Germany

Received 28 December 2005; revised 14 February 2006
Available online 9 March 2006

Abstract

It is shown how homonuclear distances and homonuclear dipolar lattice sums between spin-1/2 nuclei can be measured by a pulsed solid-state NMR experiment under magic-angle spinning conditions. The presented technique is based on double-quantum coherence filtering. Instead of measuring a build-up of double-quantum coherence the pulse sequence is designed to dephase double-quantum coherence. This is achieved by exciting double-quantum coherence either with the help of the through-space dipolar coupling or the through-bond dipolar coupling while the dephasing relies on the through-space dipolar coupling as selected by a γ-encoded pulse sequence from the C/R symmetry class. Since dephasing curves can be normalized on zero dephasing, it is possible to analyze the initial dephasing regime and hence determine dipolar lattice sums (effective dipolar couplings) in multiple-spin systems. A formula for the effective dipolar coupling is derived theoretically and validated by numerical calculations and experiments on crystalline model compounds for ^{13}C and ^{31}P spin systems. The double-quantum dephasing experiment can be combined with constant-time data sampling to compensate for relaxation effects, consequently only two experimental data points are necessary for a single distance measurement. The phase cycling overhead for the constant-time experiment is minimal because a short cogwheel phase cycle exists. A 2D implementation is demonstrated on [$^{13}C_3$]alanine.

Keywords: NMR; Solid-state; Heteronuclear homonuclear; Dipolar; Distance; *J*-coupling

1. Introduction

Spin dynamics in multiple-spin systems are known to be difficult to describe especially if quantitative information about the dipolar-interactions is of interest. To reduce the complexity of this problem only spin-1/2 systems in solid-state NMR will be considered here. The first successful approach to treat multiple spin effects is the method of moments developed by van Vleck [1] which links the lineshape function of a static sample with lattice sums of the dipolar coupling constants. Many articles have appeared since studying the structure and dynamics [2,3] of powdered samples by observing the changes in the moments of the lineshape.

Obviously it is tempting to devise similar experiments which work under magic-angle sample-spinning conditions so distance information can be used to characterize the connections between all resolved resonances. For spins with only heteronuclear dipolar couplings this is possible by an analysis of the initial part of the REDOR curve [4]. The initial part of the REDOR curve [5] is independent of the relative orientations of the through-space dipolar orientations and is a function of the individual lattice sums of dipolar couplings. To get quantifiable results it can be important to suppress the homonuclear dipolar coupling while recoupling the heteronuclear dipolar coupling as for example in PRESTO [6] or C-REDOR [7] experiments.

In the case of the homonuclear dipolar coupling many pulse methods [8–10] have been developed to isolate the homonuclear dipolar interaction. Some of these methods

* Fax: +49 89 2180 77440.
E-mail address: gunch@cup.uni-muenchen.de.

1090-7807/$ - see front matter © 2006 Elsevier Inc. All rights reserved.
doi:10.1016/j.jmr.2006.02.009

have already been applied to multiple-spin systems [11–15]. A rather successful subclass of experiments are double-quantum (DQ) filtered experiments which can be used to encode the dipolar interaction either by rotor phase modulation [16,17] or by varying the double-quantum/zero-quantum conversion times [18,19]. Rotor-phase encoded experiments were mostly applied to systems with small chemical shift anisotropies like ^{1}H containing samples [20,21] and ^{29}Si in silicates [22]. Double-quantum/zero-quantum conversion type experiments profit from the high transfer efficiencies which can be achieved by γ-encoded pulse sequences for example from the R/C-symmetry classes [23]. One aim of DQ pulse sequence design is suppression of the chemical shift while maintaining a high scaling-factor for the dipolar interaction. Again solutions can be found in the class of R/C-sequences [23].

The analysis of the spin-dynamics of a multiple-spin system under such a DQ Hamiltonian is difficult [24–26]. For ^{1}H NMR it was suggested that the linewidth under magic-angle-spinning conditions can be analyzed in terms of dipolar lattice sums [27]. In DQ/ZQ conversion type experiments (ZQ for zero-quantum) the initial regime of a DQ build-up curve does not depend on the relative orientations of the dipolar interactions, which opens the possibility to measure a well defined dipolar lattice value for every resolved DQ coherence [28,29,13]. However a numerically stable analysis of the experimental data without normalization [13] of the DQ intensities is critical and can be hampered by relaxation and interference from *J*-couplings.

The pulse sequences presented here are based on the DQ/ZQ conversion approach. Instead of sampling the build up of DQ coherence [30] the pulse sequences are designed to follow the dephasing of DQ coherence under a DQ Hamiltonian. DQ coherence can either be excited with the help of the through-space or the through-bond dipolar interaction as in the INADEQUATE experiment [31,32]. Hence it is possible to make use of the through-space dipolar coupling and the through-bond dipolar coupling in a single experiment which resembles the situation in the double-filter DQ constant-time experiment [33]. Compensation for relaxation and experimental imperfections can be achieved following the ideas of DQ constant-time NMR [33–36].

The article is organized into several sections. In Section 2, the pulse sequences are described in detail, including phase cycling tables and pulse timings. In Section 3, the spin-dynamics of double-quantum dephasing are treated theoretically and the connections to dipolar lattice sums and the degree of isotopic labelling are established. In the following section experimental results are presented and discussed.

2. Pulse-sequences

Pulse sequences for double-quantum coherence dephasing (Double-Quantum Dephasing, DoDe) are sketched out in Fig. 1. The pulse sequences are similar to ordinary zero-quantum filtered DQ NMR. In a first step DQ coherence is created by a pulse block generating a DQ average Hamiltonian either based on the through-bond or on the through-space dipolar interaction. In this contribution in the theoretical part only γ-encoded pulse sequences from the *C*/*R* symmetry classes are considered for the latter case. All experimental results were obtained with the PostC7 sequence [19], i.e., $C7_2^1$ with the C-element 90_0–360_{180}–270_0. The *J*-coupling based sequence is using the echo-type hard pulse excitation of the liquid-state INADEQUATE [32] experiment. The three pulse 90_0–$\tau_{DQ}^J/2$–180_{90}–$\tau_{DQ}^J/2$–90_0 sequence will henceforth be called "INADEQUATE block," where x_y describes a pulse with a flip angle of x degrees and a pulse phase of y degrees. The timing τ_{DQ}^J has to be chosen such that the centres of the 90° and 180° pulses are separated by an integer multiple of the rotor period.

The DQ excitation is followed by one (pulse sequence B) or two dephasing periods (pulse sequence A and C) using a pulse sequence from the *C*/*R* symmetry class, here PostC7 [19]. The PostC7 sequence interconverts elements of the density matrix with even coherence orders, for short dephasing periods τ_1 and τ_2 mostly DQ and ZQ coherences. Coherence transfer pathways are suppressed by the phase cycle if the PostC7 sequence has induced a change in coherence order after the dephasing periods. In the constant-time experiments (pulse sequence A and C) this procedure is repeated twice.

After the dephasing period the DQ coherence is reconverted to zero-quantum coherence again using the INADEQUATE block or a C-/R-type pulse sequence, respectively. The length of the dephasing times τ_1, τ_2 and the excitation and reconversion times τ_{exc} and τ_{recon} can be adjusted by repeating blocks of complete $C7_2^1$ cycles several times. Consequently the pulse sequence and the sampling of the DQ dephasing curves is done in a rotor synchronized manner. Finally a 90° pulse generates transverse magnetization.

Coherence pathway selection was achieved by phase cycling the pulse phases only, thus keeping the receiver phase constant. The constant-time DQ dephasing sequences consist of five blocks excitation, dephasing-I, dephasing-II, reconversion, and read pulse. To the phases of all pulses in each block a phase ϕ_{block}^i is added, where i refers to the ith experiment. The five phases ϕ_{exc}^i, $\phi_{dephasing\text{-}I}^i$, $\phi_{dephasing\text{-}II}^i$, ϕ_{recon}^i and ϕ_{read}^i were chosen according to a cogwheel phase cycle [37]. The shortest possible cogwheel phase cycle requires at least 36 experiments to be added up. The differences in winding numbers are then $\Delta\nu_{12} = 3$, $\Delta\nu_{23} = 3$, $\Delta\nu_{34} = 3$, and $\Delta\nu_{45} = 1$ for the consecutive, independently cycled blocks, which amounts to a Cog36(8,11,14,17,18;0). Thus the pulse phase increments ϕ_{block}^i in the ith experiment are:

i	1	2	3	4	5	6	7	8	9	10	11	12	13	14	15	16	17	18
ϕ^i_{exc}	0.0	80.0	160.0	240.0	320.0	40.0	120.0	200.0	280.0	0.0	80.0	160.0	240.0	320.0	40.0	120.0	200.0	280.0
$\phi^i_{\text{dephasing-I}}$	0.0	110.0	220.0	330.0	80.0	190.0	300.0	50.0	160.0	270.0	20.0	130.0	240.0	350.0	100.0	210.0	320.0	70.0
$\phi^i_{\text{dephasing-II}}$	0.0	140.0	280.0	60.0	200.0	340.0	120.0	260.0	40.0	180.0	320.0	100.0	240.0	20.0	160.0	300.0	80.0	220.0
ϕ^i_{recon}	0.0	170.0	340.0	150.0	320.0	130.0	300.0	110.0	280.0	90.0	260.0	70.0	240.0	50.0	220.0	30.0	200.0	10.0
ϕ^i_{read}	0.0	180.0	0.0	180.0	0.0	180.0	0.0	180.0	0.0	180.0	0.0	180.0	0.0	180.0	0.0	180.0	0.0	180.0
i	19	20	21	22	23	24	25	26	27	28	29	30	31	32	33	34	35	36
ϕ^i_{exc}	0.0	80.0	160.0	240.0	320.0	40.0	120.0	200.0	280.0	0.0	80.0	160.0	240.0	320.0	40.0	120.0	200.0	280.0
$\phi^i_{\text{dephasing-I}}$	180.0	290.0	40.0	150.0	260.0	10.0	120.0	230.0	340.0	90.0	200.0	310.0	60.0	170.0	280.0	30.0	140.0	250.0
$\phi^i_{\text{dephasing-II}}$	0.0	140.0	280.0	60.0	200.0	340.0	120.0	260.0	40.0	180.0	320.0	100.0	240.0	20.0	160.0	300.0	80.0	220.0
ϕ^i_{recon}	180.0	350.0	160.0	330.0	140.0	310.0	120.0	290.0	100.0	270.0	80.0	250.0	60.0	230.0	40.0	210.0	20.0	190.0
ϕ^i_{read}	0.0	180.0	0.0	180.0	0.0	180.0	0.0	180.0	0.0	180.0	0.0	180.0	0.0	180.0	0.0	180.0	0.0	180.0

The phase cycle selects the coherence transfer pathways $0 \to +2 \to +2 \to +2 \to 0 \to -1$ and $0 \to -2 \to -2 \to -2 \to 0 \to -1$ as indicated in Fig. 1 (pulse sequences A and C), neglecting all coherence pathways which involve coherence orders $|p| > 2$. An additional 4-step phase cycle realizes DC offset and quadrature image compensation. The phase cycling becomes significantly shorter through the choice of the cogwheel phase cycle. A nested phase cycle which would select the same coherence transfer pathways would need 240 steps.

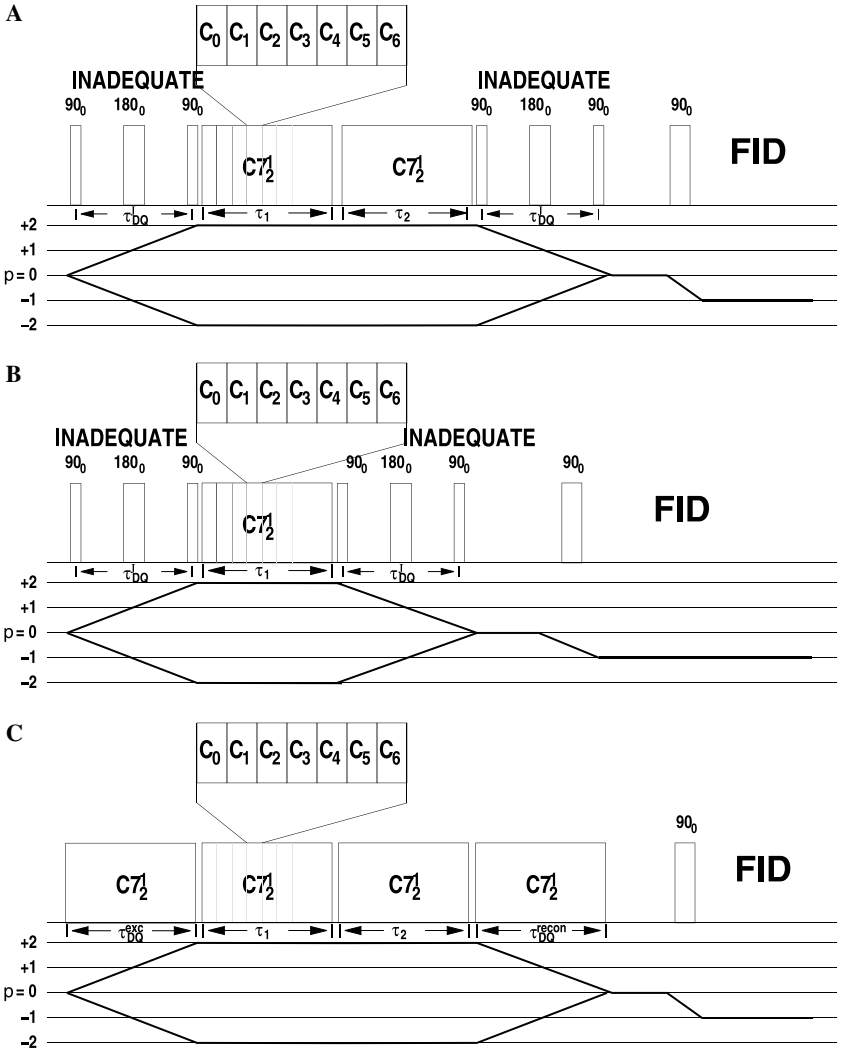

Fig. 1. Pulse sequences for measuring double-quantum dephasing curves. (A) Constant-time dephasing of double-quantum coherences generated via J-couplings using an INADEQUATE pulse scheme, (B) non-constant-time version of (A), (C) constant-time dephasing of double-quantum coherences generated with a PostC7 sequence.

For reasons of convenience the DQ dephasing experiment with a single dephasing period (pulse sequence B, Fig. 1) was realized with the same pulse sequence and phase cycling, only one of the dephasing periods was set to zero.

3. Theory

3.1. Two-spin system

The double-quantum filtered intensity can be written as a function of the dephasing time τ, throughout which the double-quantum Hamiltonian is applied (pulse sequence B, Fig. 1). The contribution of different crystallites in a powder to the filtered signal is almost independent of their orientation if an INADEQUATE experiment under fast spinning conditions is used for the double-quantum to zero-quantum conversion steps. Consequently the analysis of spin-dynamics for the complete sequence is significantly simplified. On the other hand the isotropic approximation requires a fast spinning-regime to suppress the anisotropic parts of chemical shift and the through-space dipolar coupling during the INADEQUATE blocks of the pulse experiment.

With the first-order effective Hamiltonian $\bar{\mathcal{H}}^{(1)}_{lm\lambda\mu}$ of a γ-encoded *C*- or *R*-pulse sequence [23,38,26] the filtered double-quantum intensity S_{DQ} becomes

$$S_{\mathrm{DQ}}(\tau) \propto \left\langle \frac{1}{2} + \frac{1}{2}\cos(|\omega_{12}|\tau) \right\rangle \tag{1}$$

for a single spin-pair where $\langle\cdots\rangle$ denotes the powder average. The frequency ω_{12} refers to the scaled dipolar coupling constant in the first order average Hamiltonian $\bar{\mathcal{H}}^{(1)}_{lm\lambda\mu}$ and its magnitude $|\omega_{12}|$ to $\sqrt{\omega_{12}\omega^*_{12}}$. In a multiple spin system it is the sum of the double-quantum terms obtained from all pairwise combinations of nuclei. For a PostC7 pulse train it takes the form

$$\bar{\mathcal{H}}^{(1)}_{lm\lambda\mu} = \sum_{j\neq k}^{jk} \left(\omega_{jk} T^{jk}_{2-2} + \omega^*_{jk} T^{jk}_{22} \right), \tag{2}$$

where $T^{jk}_{2\pm2}$ are second rank spin operators for the interaction between spins j and k and where the terms $(l,m,\lambda,\mu) = (2,-1,2,2)$ and $(2,1,2,-2)$ are selected by the pulse sequence symmetry (here $C7^1_2$). Here l and m are space rank and component while λ and μ refer to spin rank and component of the recoupled interaction. Details are described in the literature [30]. The factor ω_{jk} is proportional to the product of the complex scaling factor $\kappa_{lm\lambda\mu}$ [26] and the dipolar coupling constant ν_{dip}

$$\nu_{\mathrm{dip}} = -\frac{\mu_0}{8\pi^2}\gamma^2\hbar/d^3, \tag{3}$$

where d is the internuclear distance and γ is the magnetogyric ratio. Explicitly the frequency ω_{jk} can be written out as [26]

$$\omega_{jk} = \sqrt{24}\nu_{\mathrm{dip}}\pi\kappa_{lm\lambda\mu} e^{i(\alpha_{\mathrm{RL}}+\gamma_{\mathrm{MR}})} \times \sum_{m=-2}^{+2} d^2_{0m}(\beta^{jk}_{\mathrm{PM}}) d^2_{m-1}(\beta_{\mathrm{MR}}) e^{-im(\gamma_{\mathrm{PM}}+\alpha_{\mathrm{MR}})} \tag{4}$$

assuming rotorsynchronized application and a zero starting phase of the rf-pulse train. Here the Euler angles α_{PM}, β_{PM}, γ_{PM} describe a rotation from the principle axis frame of the homonuclear dipolar interaction to the molecular frame, the Euler angles α_{MR}, β_{MR}, γ_{MR} the rotation from the molecular frame to the rotor frame and Euler angles α_{RL}, β_{RL}, γ_{RL} describe a rotation from the rotor to the laboratory frame. For a single dipolar interaction the molecular frame may be chosen such that the molecular frame and the principal axes frame coincide and the relevant Euler angles α_{PM}, β_{PM}, γ_{PM} become zero. For this case Eq. (4) simplifies to

$$\omega_{jk} = -3\pi\nu_{\mathrm{dip}}\kappa_{2-122}\sin(2\beta_{\mathrm{MR}})e^{i(\alpha_{\mathrm{RL}}+\gamma_{\mathrm{MR}})}. \tag{5}$$

Ideally, a DQ dephasing experiment can be performed with a single variable dephasing time. Then a dipolar coupling constant can be extracted from the observed oscillations of DQ intensity as a function of dephasing time in a similar way as for a double-quantum build-up curve. The main advantage of a dephasing technique is that it can be normalized which means that short dephasing times can be analyzed for dipolar couplings. Normalization can be achieved by taking the quotient of the dephased intensity $S_{\mathrm{DQ}}(\tau)$ over the intensity $S_{\mathrm{DQ}}(0)$ of an experiment without dephasing. The ratio can be fitted with a dipolar coupling constant. Knowledge about the isotropic *J*-coupling constant is not necessary, because its influence onto DQ-dephasing is negligible in most cases. On the other hand relaxation can be suspected to corrupt the experiment because it acts as an additional mechanism which lowers the DQ filtered intensity.

Relaxation effects can often be minimized by using a constant-time setup [33–35]. For this purpose the dephasing block is split into two separate periods τ_1 and τ_2. The dephasing of DQ-coherence after a total dephasing time τ_{total} does not depend on the choice of τ_1 and τ_2 as long as the overall dephasing time is kept constant ($\tau_1+\tau_2=\tau_{\mathrm{total}}$, see pulse-sequence A, Fig. 1), if the decay is governed by a simple exponential relaxation function. The decay caused by the dipole–dipole interaction however does depend on the choice of τ_1 and τ_2. Normalization can be achieved by taking the ratio of two experiments with equal total dephasing time τ_{total}. To achieve maximum difference of their double-quantum filtered intensities S_{DQ} the dephasing periods τ_1 and τ_2 were chosen as ($\tau_1=0$, $\tau_2=\tau_{\mathrm{total}}$) and ($\tau_1=\frac{\tau_{\mathrm{total}}}{2}, \tau_2=\frac{\tau_{\mathrm{total}}}{2}$).

$$\frac{S_{\mathrm{DQ}}(\tau_1=0,\tau_2=\tau_{\mathrm{total}})}{S_{\mathrm{DQ}}(\tau_1=\frac{\tau_{\mathrm{total}}}{2},\tau_2=\frac{\tau_{\mathrm{total}}}{2})} = \frac{\left\langle 1\cdot\left(\frac{1}{2}+\frac{1}{2}\cos\left(|\omega_{12}|\tau_{\mathrm{total}}\right)\right)\right\rangle}{\left\langle\left(\frac{1}{2}+\frac{1}{2}\cos\left(|\omega_{12}|\frac{\tau_{\mathrm{total}}}{2}\right)\right)\left(\frac{1}{2}+\frac{1}{2}\cos\left(|\omega_{12}|\frac{\tau_{\mathrm{total}}}{2}\right)\right)\right\rangle}. \tag{6}$$

Only two experimental values are necessary to determine a single dipolar coupling. In analogy with double-quantum constant-time experiments [35] there exists an upper limit $|\nu^{\max}_{\mathrm{dip}}|$ up to which dipolar coupling constants can unambiguously be characterized for a given dephasing period τ_{total}

and a given scaling factor κ. The upper limit $|\nu_{\mathrm{dip}}^{\max}|$ can be approximated from the first minimum in the integrated Taylor expansion to the 6*th* order of the above formula as $|\nu_{\mathrm{dip}}^{\max}| \approx \frac{0.3558}{\tau_{\mathrm{total}}|\kappa|}$. From the same expansion (see supporting information) a good numerical approximation of the dephasing curve with a given dipolar coupling constant ν_{dip} and a given scaling factor κ can be calculated. Alternatively the following integral can be evaluated numerically:

$$S_{\mathrm{DQ}}^{\mathrm{CT}}(\tau) = \frac{S_{\mathrm{DQ}}(\tau_1 = 0, \tau_2 = \tau_{\mathrm{total}})}{S_{\mathrm{DQ}}(\tau_1 = \frac{\tau_{\mathrm{total}}}{2}, \tau_2 = \frac{\tau_{\mathrm{total}}}{2})} = \frac{\int_0^{\pi}(\frac{1}{2} + \frac{1}{2}\cos(3|\kappa|\nu_{\mathrm{dip}}\pi\tau_{\mathrm{total}}\sin(2\beta_{\mathrm{MR}}))\sin(\beta_{\mathrm{MR}})\,\mathrm{d}\beta_{\mathrm{MR}}}{\int_0^{\pi}\left(\frac{1}{2} + \frac{1}{2}\cos\left(\frac{3}{2}|\kappa|\nu_{\mathrm{dip}}\pi\tau_{\mathrm{total}}\sin(2\beta_{\mathrm{MR}})\right)\right)^2\sin(\beta_{\mathrm{MR}})\,\mathrm{d}\beta_{\mathrm{MR}}}. \quad (7)$$

The quality of the expansion can be assessed from comparison with the numerical integration of the analytic formula based on an averaged Hamiltonian and from comparison with the exact numerical calculations of the spin-dynamics in a two-spin system (see Fig. 2).

3.2. Multiple-spin system

The effective Hamiltonian for a huge spin-1/2 system consists of a sum of double-quantum terms. The double-quantum coherence $I_{\pm i}I_{\pm j}$ of the nuclei i and j in a multiple-spin system will dephase under the double-quantum averaged Hamiltonian with contributions from all spin-pairs in the multiple-spin system.

Contributions of different spin-pairs with one common spin do not commute which each other in general. Hence it is not possible to apply them consecutively to the density matrix as the individual heteronuclear dipolar interactions in a REDOR experiment [39]. The oscillation of a double-quantum build-up curve carries information not only about the dipolar coupling constants but also about their relative orientation [24]. In the Baker–Campbell–Hausdorff the orientational dependence appears in form of the commutators in the series expansion.

$$\mathrm{e}^{\mathrm{i}H_A\tau}\mathrm{e}^{\mathrm{i}H_B\tau} = \mathrm{e}^{\mathrm{i}(H_A+H_B)\tau - \frac{1}{2}[H_A,H_B]\tau^2 + \cdots}. \quad (8)$$

For short conversion times the Baker–Campbell–Hausdorff equation may be truncated after the first term, because all commutators are scaled by higher powers of τ.

$$\mathrm{e}^{\mathrm{i}H_A\tau}\mathrm{e}^{\mathrm{i}H_B\tau} \approx \mathrm{e}^{\mathrm{i}(H_A+H_B)\tau}. \quad (9)$$

Short in this context means $1/\tau \gg H_{ii}$. In this approximation the double-quantum average Hamiltonian can be split into factors of individual two-spin double-quantum terms. There are three categories of dephasing by two-spin double-quantum terms: terms $I_{\pm k}I_{\pm l}$ with no spin in common with the indirectly observed double-quantum coherence $I_{\pm i}I_{\pm j}$, terms $I_{\pm i}I_{\pm k}$ with one spin in common (Eq. (10)) and terms $I_{\pm i}I_{\pm k}$ with two spins in common (Eq. (11)) as discussed in the section "two-spin system" above. Since double-quantum terms for coherences with no spin in common commute with $I_{\pm i}I_{\pm j}$, there are only two types of contributions left, which have an impact onto the initial part of the dephasing curve:

$$I_{+i}I_{+j} \xrightarrow{\omega_{jk}T_{2-2}^{jk} + \omega_{jk}^{*}T_{22}^{jk}} \cos\left(\frac{1}{2}|\omega_{jk}|\tau\right)I_{+i}I_{+j}, \quad (10)$$

$$I_{+i}I_{+j} \xrightarrow{\omega_{ij}T_{2-2}^{ij} + \omega_{ij}^{*}T_{22}^{ij}} \cos^2\left(\frac{1}{2}|\omega_{ij}|\tau\right)I_{+i}I_{+j}. \quad (11)$$

For short dephasing times the intensity $S_{\mathrm{DQ}}(\tau)$ is proportional to the product of the contributions of all dephasing double-quantum terms. All irrelevant constant prefactors can be removed by normalizing to the filtered signal intensity S_{DQ} at $\tau = 0$ (pulse sequence B in Fig. 1).

$$S_{\mathrm{DQ}}(\tau)/S_{\mathrm{DQ}}(0) = \left\langle \prod_{ij,i\neq j} \cos\left(\frac{1}{2}|\omega_{ij}(\alpha_{\mathrm{MR}},\beta_{\mathrm{MR}},\gamma_{\mathrm{MR}})|\tau\right)\right\rangle. \quad (12)$$

A cosine expansion $\cos x = 1 - \frac{x^2}{2!} + \frac{x^4}{4!} + \cdots$ results in

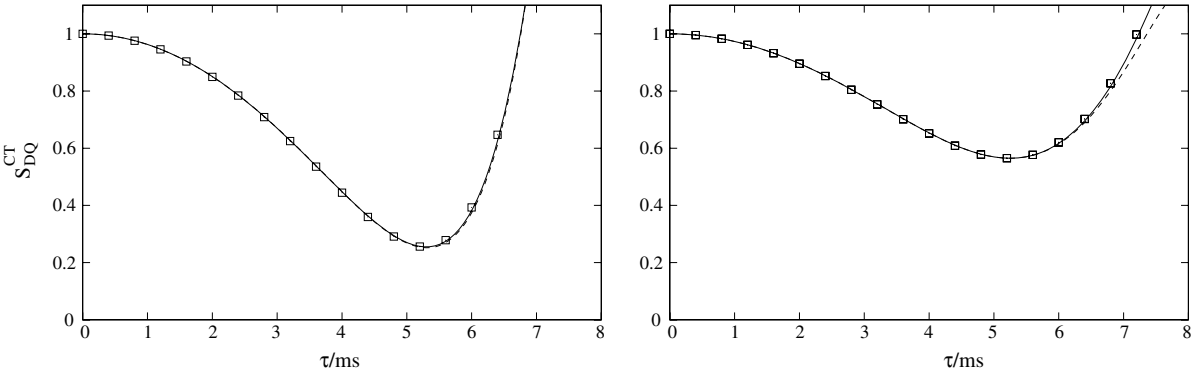

Fig. 2. The constant-time double-quantum dephasing ratio $S_{\mathrm{DQ}}^{\mathrm{CT}}$ as a function of the dephasing time τ_{total} using PostC7 for dephasing and an INADEQUATE block (right diagram, pulse sequence A in Fig. 1) or PostC7 (left diagram, pulse sequence C in Fig. 1) for DQ generation, respectively; squares refer to numerically exact 2-spin simulations for a dipolar coupling constant of $\nu_{\mathrm{dip}} = -436$ Hz, the dashed line was obtained using the series expansion to the 10th order (see supporting material) of the dephasing functions and the solid line was obtained via numerical integration of the dephasing functions in Eqs. (7) and (16).

$$S_{DQ}(\tau)/S_{DQ}(0) = \frac{1}{8\pi^2}\int_0^{2\pi} d\alpha_{MR}\int_0^{\pi}\sin\beta_{MR}\,d\beta_{MR} \times \int_0^{2\pi} d\gamma_{MR}\prod_{ij}\left[1-\frac{1}{8}\left(|\omega_{ij}(\alpha_{MR},\beta_{MR},\gamma_{MR})|\tau\right)^2+\cdots\right]. \quad (13)$$

The expansion is truncated after the second term (in the limit $x \ll 1$) and the product is expanded. Again for short dephasing times all terms with an order higher than 2 are neglected and for the same reason spin-products like $(\omega_{ij}(\alpha_{ij},\beta_{ij},\gamma_{ij})\tau)^2(\omega_{kl}(\alpha_{kl},\beta_{kl},\gamma_{kl})\tau)^2$. A simple sum of squared dipolar couplings is factored out

$$S_{DQ}(\tau)/S_{DQ}(0) \approx \frac{1}{8\pi^2}\int_0^{2\pi} d\alpha_{MR}\int_0^{\pi}\sin\beta_{MR}\,d\beta_{MR} \times \int_0^{2\pi} d\gamma_{MR}\left[1-\frac{1}{8}\tau^2\sum_{ij}\left|\omega_{ij}(\alpha_{MR},\beta_{MR},\gamma_{MR})\right|^2\right]. \quad (14)$$

The formula is an approximation of the beginning of the dephasing curve. The integral can readily be evaluated because there are no cross products of different pairwise dipolar couplings, which would make the dephasing curve dependent on relative orientations. The absence of cross products also removes the dependence on the Euler angles relating the individual dipolar interactions in the principal axis and the molecular frame. Using Eqs. (3) and (4) a sum of squared dipole–dipole coupling constants can be factored out, which determines how quickly double-quantum coherence is being dephased.

The experimentally observable quantity extrapolated to zero dephasing time is equivalent to a dipolar coupling constant ν_{eff} (alias effective dipolar coupling) in a fictitious 2-spin system. The effective dipolar coupling constant can quickly be calculated from a sum of squared dipolar coupling constants. It is well defined for any given crystal structure by the internuclear distances of the dipolarly coupled nuclei.

$$\nu_{eff} = -\frac{1}{\sqrt{2}}\sqrt{\sum_{1i,i\neq 1}^{\text{nuclei}}\nu_{1i}^2+\sum_{2i,i\neq 2}^{\text{nuclei}}\nu_{2i}^2}. \quad (15)$$

The effective dipolar coupling is converging quickly with distance. The dipolar coupling belonging to the observed DQ coherence occurs twice in the formula for effective dipolar coupling, once for each nucleus in the observed DQ coherence. Similar results have been found for the excitation behaviour of DQ build-up curves [26,40,41,28].

Numerical calculations of the spin-dynamics of 2- to 7-spin systems have been performed including all dipolar couplings to determine the regime in which the effective dipolar coupling constant serves as a good approximation. The dipolar coupling network including all the relative orientations refers to the crystal structure of $Ag_7P_3S_{11}$ at room temperature [42]. The observed spin-pair belongs to the two inequivalent P-atoms in the $P_2S_7^{4-}$ anion. The effective dipolar coupling constant and the dephasing ratio is plotted against the dephasing time (see Fig. 3). The effective dipolar coupling constant, determined from the dephasing ratio at short dephasing time, correlates very well with an effective dipolar coupling that was obtained by summing up the appropriate dipolar couplings as shown in Eq. (15) (see Fig. 3).

For short dephasing times the effective dipolar coupling constant is in good agreement with the expected values. The plots in Fig. 3 indicate that intensity ratios to about

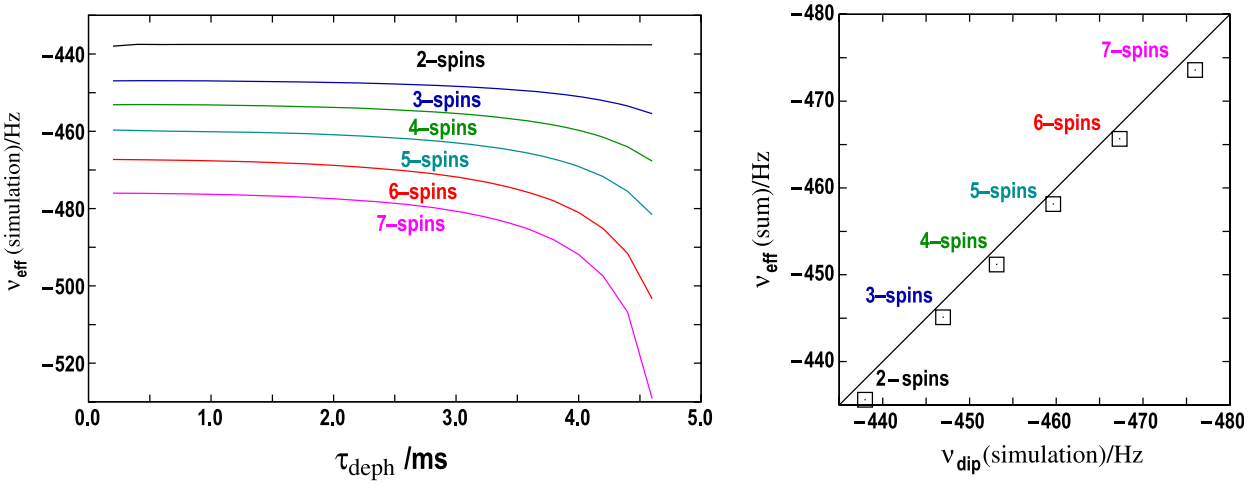

Fig. 3. Effect of multiple-spins on effective dipolar coupling constants measured from dipolar dephasing ratios; left: effective dipolar coupling constants ν_{eff}(simulation) in multiple spin systems as a function of dephasing time τ_{deph}, determined from numerically accurate simulations of the spin dynamics; right: the effective dipolar coupling constant ν_{eff}(sum) calculated with formula (15) plotted against the effective dipolar coupling constant ν_{eff}(simulation) determined via the dephasing ratio from numerically accurate simulations of the spin dynamics; calculations were set up for the ^{31}P spins in crystalline $Ag_7P_3S_{11}$ including all isotropic chemical shifts, J-couplings and all dipole–dipole interactions (magnitude and orientation were taken from the crystal structure).

70% give meaningful effective dipolar coupling constants in case of crystalline $Ag_7P_3S_{11}$. Small differences of 2–3 Hz can be traced back to the chemical shift offset dependence of the PostC7 pulse sequence.

These formulas neglect anisotropic *J*-coupling and relaxation. The concept of the effective dipolar coupling also applies to the constant-time version since the dephasing in a multiple-spin system under pulse sequence A (see Fig. 1) can be described essentially in the same way as in the case of pulse sequence B.

3.3. DQ dephasing with through-space dipolar coupling mediated DQ excitation

An interesting aspect of the effective dipolar coupling is that it is a simple sum of all dipole–dipole couplings of the two observed spin-1/2 nuclei. The dipole–dipole coupling between the two observed spin-1/2 nuclei has no extra impact onto the initial dephasing function as compared to all the other dipole–dipole couplings. This means that the requirement for a *J*-coupling mediated DQ-excitation-mechanism can be dropped and the through-space coupling can also be used for the conversion of zero-quantum to double-quantum coherence and vice versa.

A suitable pulse-sequence is described in Fig. 1 (pulse sequence C). The *J*-mediated conversion blocks are simply exchanged by PostC7 blocks. But also any other pulse train would be possible which would lead to γ-encoded DQ excitation via the through-space dipole–dipole coupling. The constant-time approach and the phase cycling increments of the individual blocks are identical to those in pulse sequence A in Fig. 1.

A major difference to the *J*-mediated double-quantum dephasing experiment is that the DQ dephasing curve (see Fig. 2) becomes dependent on the length of the excitation and reconversion times (see τ_{exc} and τ_{recon} in Fig. 1 pulse sequence C). While the analytical formula for a 2-spin system becomes slightly more complicated (assumption $\tau_{recon} = \tau_{exc}$)

$$S_{DQ}^{CT}(\tau_{total}) = \frac{S_{DQ}(\tau_1 = 0, \tau_2 = \tau_{total})}{S_{DQ}(\tau_1 = \frac{\tau_{total}}{2}, \tau_2 = \frac{\tau_{total}}{2})} = \frac{\left\langle 1 \cdot (\frac{1}{2} + \frac{1}{2}\cos(|\omega_{12}|\tau_{total}))\sin^2(|\omega_{12}|\tau_{exc})\right\rangle}{\left\langle (\frac{1}{2} + \frac{1}{2}\cos(|\omega_{12}|\frac{\tau_{total}}{2}))(\frac{1}{2} + \frac{1}{2}\cos(|\omega_{12}|\frac{\tau_{total}}{2}))\sin^2(|\omega_{12}|\tau_{exc})\right\rangle} \quad (16)$$

the analysis of the experimental dephasing ratio in terms of dipolar coupling constants for a two spin-system (see Fig. 2) remains the same. This way of conducting a constant-time DQ experiment has the advantage of a more efficient dephasing down to dephasing ratios of about 25%. Consequently for identical dephasing times τ_{total} for pulse sequences A and C the dephasing ratio is less effected by noise in the latter, hence the error of the experimental effective dipolar coupling is significantly smaller. Explicit formulas for the integrated dephasing curve are given in the supporting information.

In a multiple spin system n-spin double-quantum coherences have to be taken into account if the conversion times τ_{exc} or τ_{recon} become too long. This case might occur if in a sample both weakly coupled and strongly coupled spin-pairs are under investigation. Then n-spin double-quantum coherences can cause extra dephasing, such that Eq. (15) for the effective dipolar coupling of the observed spins is no longer a good approximation. However for short conversion times τ_{exc} or τ_{recon} the analysis of the dephasing behaviour in terms of an effective dipolar coupling is possible.

3.4. Uniformly isotopically enriched samples

In uniformly isotopically enriched samples the effective dipolar coupling is a function of the degree of isotopic enrichment *p* [43]. Especially in organic compounds the level of enrichment of ^{13}C, ^{1}H, and ^{15}N can often be controlled experimentally. The level of enrichment *p* has a big influence on the effective dipolar coupling constant. An interesting situation occurs if the through-bond dipolar coupling is chosen for the excitation of DQ coherence. Take the example of a partially ^{13}C labelled crystalline alanine sample. The C-atoms belonging to the observed DQ coherence have to be ^{13}C, but for all other carbon atoms the chances of being ^{13}C and not ^{12}C are lower and given by the probability *p*. Like in a lottery most DQ ^{13}C-atom spin-pairs will have different patterns of NMR active neighbouring C-atoms, called configuration, and hence differing effective dipolar coupling constants. Then the observed experimental dephasing ratio $\overline{S_{DQ}^{CT}}$ is the statistical average over the individual dephasing ratios of the configurations in a powder.

$$\overline{S_{DQ}^{CT}} = \lim_{n\to\infty} \frac{\sum_i^n S_{DQ}^{CT}(i)}{n}.$$

In this complex situation we can again resort to the initial regime of the DQ dephasing curve. The most important contribution to the initial part is quadratic in dephasing time and the effective dipolar coupling constant. An approximation can be derived for the effective dipolar coupling constant $\nu_{eff}(p)$ of an observed spin-pair in a crystal with the dipolar coupling constant ν_{12}. The two limiting cases $p = 0$ and $p = 1$ refer to the isolated two-spin case and the effective dipolar coupling constant ν_{eff} as described in Eq. (15) for full enrichment, respectively

$$\nu_{eff}(p) \approx -\sqrt{\nu_{12}^2 + \frac{p}{2}\left(\sum_{\substack{i\neq 1,\neq 2\\ 1i}}^{\text{nuclei}} \nu_{1i}^2 + \sum_{\substack{i\neq 1,\neq 2\\ 2i}}^{\text{nuclei}} \nu_{2i}^2\right)}. \quad (17)$$

Only the dipolar couplings to spins not belonging to the observed spin-pair depend on the degree of enrichment *p*. The relationship may serve to get an estimate for the error of ν_{12} in isotopically enriched samples. If samples can be isotopically enriched such that randomly all positions have the same degree of enrichment *p* it is possible to calculate

the dipolar coupling for the observed spin-pair v_{12} from the effective dipolar coupling constants $v_{\mathrm{eff}}(p)$ at two different levels of enrichment.

4. Results and discussion

The double-quantum dephasing experiment is yet another experiment for measuring homonuclear dipolar couplings. In contrast to build-up curve based experiments the idea is to dephase DQ coherence. Like in the REDOR experiment good signal to noise ratios can be achieved even for short dephasing times and normalization is feasible. The DQ evolution time necessary to encode the same dipolar coupling is shorter for DQ dephasing experiments than for DQ experiments based on build-up curves. In a constant-time DQ dephasing experiment for example at least 1.6 ms total dephasing time are necessary to encode the P-P distance of the P_2S_7 group in $Ag_7P_3S_{11}$, while in an experiment based on build-up curves at least 5.6 ms are necessary [35]. The advantages of DQ dephasing come at the cost of a slightly longer phase cycle. In ordinary DQ filtered experiments a phase cycle with 12 steps has to be completed to select a coherence order pathway of $0 \rightarrow \pm 2 \rightarrow 0 \rightarrow -1$. In constant time DQ-dephasing experiments 36 steps are necessary.

In the short dephasing time limit it is possible to analyze the behaviour of multiple-spin systems. The effective dipolar coupling as defined in Eq. (15) is an approximation for the initial part of the DQ dephasing curve in multiple spin systems and needs to be validated against experimental evidence. In Fig. 4 the experimental value of the effective dipolar coupling is shown as a function of dephasing time for the ^{31}P resonances of the P_2S_7-group in crystalline $Ag_7P_3S_{11}$. As a theoretical reference serve the spin-pair dipolar coupling constant of the P-atoms in the P_2S_7-group and the corresponding effective dipolar coupling constant v_{eff} as calculated from the crystal structure (dashed and solid horizontal lines in Fig. 4).

Random errors of the effective dipolar couplings were determined from the approximated error of experimental DQ-filtered intensities via error propagation. A small random error in intensity results in a big random error for the first data points. However already with about 1 ms of dephasing time the random errors become tolerable in the case of $Ag_7P_3S_{11}$.

The three dephasing curves in Fig. 4 allow a comparison of the three pulse sequences in Fig. 1. For the simple DQ-dephasing sequence (pulse sequence B, Fig. 1) a systematic deviation of almost 200 Hz can be observed, while for both constant-versions of the DQ-dephasing experiments (pulse sequences A and C, Fig. 1) the experimental values agree with the theoretical predictions within experimental error. For the latter this corresponds to dephasing ratios down to 78% and 65%, respectively. This indicates that the anisotropic J-coupling constant is much smaller than the through space dipolar coupling. The better overlap between experimental and predicted values indicates that constant-time sampling efficiently removes relaxation and experimental deficiencies of the simple dephasing experiment (pulse sequence B). For the case of $Ag_7P_3S_{11}$ the approximations in theory seem to be valid, since the effective dipolar couplings agree to the predicted effective dipolar couplings up to dephasing times $\tau = 2.5$ ms. The experimental conditions described for $Ag_7P_3S_{11}$ should be relevant for ordinary oxidic diphosphates.

DQ-dephasing can be implemented in a two-dimensional experiment by inserting an evolution time between the second block of DQ dephasing and DQ reconversion, which results in a 2D double-quantum single-quantum correlation spectrum after a 2D Fourier-transformation. This adds the resolution power of a 2D experiment to the distance determination capabilities of the constant-time DQ-dephasing experiment. If the observed DQ coherences represent similar internuclear distances, two 2D spectra, that are acquired with the dephasing times chosen as detailed above, are sufficient to determine the complete set of dipolar coupling constants or the effective dipolar coupling constants, respectively. In Fig. 5 a ^{13}C NMR 2D DQ-dephasing spectrum is shown for crystalline [$^{13}C_3$]alanine with a

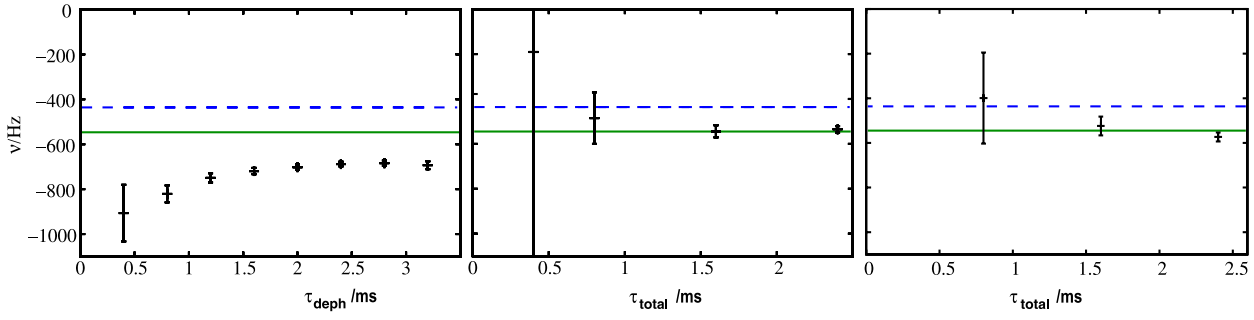

Fig. 4. Experimental values of the effective dipolar coupling as a function of dephasing time for the ^{31}P DQ coherence for phosphorus atoms in P_2S_7, the data were acquired at a sample rotation frequency of 10 kHz; left: simple dephasing (pulse sequence B in Fig. 1), constant-time DoDe using J-couplings for excitation and reconversion (pulse sequence A in Fig. 1, $\tau'_{\mathrm{DQ}} = 20$ ms), constant-time DoDe using the direct dipole–dipole coupling for excitation and reconversion (pulse sequence C in Fig. 1, $\tau_{\mathrm{recon}} = \tau_{\mathrm{exc}} = 1.6$ ms); the dashed horizontal lines refer to the dipolar coupling constant between the two P-atoms in the P_2S_7 group and solid horizontal lines to the effective dipolar coupling constant referring to the dipolar interactions of all P-atoms in the $Ag_7P_3S_{11}$ crystal.

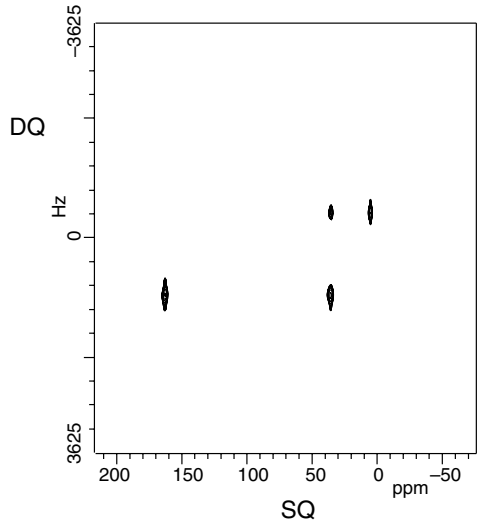

Fig. 5. Double-quantum filtered 2D correlation spectrum of [$^{13}C_3$]alanine acquired with a DoDe pulse sequence (pulse sequence B in Fig. 1); no distortions of the line shape were observed; total dephasing time $\tau_{total} = 551.72\ \mu s$, $\tau'_{DQ} = 1517.24\ \mu s$, $\nu_r = 7250$ Hz.

Table 1
Dipolar coupling constants: effective dipolar coupling constants ν_{eff} calculated from the crystal structures [50,51], experimental values ν_{exp} and for comparison the dipolar coupling constants ν_{dip} for a given spin-pair; the experimental values refer to pulse sequence A in Fig. 1

Compound	Atoms	ν_{eff} (Hz)	ν_{dip} (Hz)	ν_{exp} (kHz)
$Ag_7P_3S_{11}$	$P_2S_7^{4-}$	−545	−436	−0.535
Alanine	$^{13}C_\alpha$–$^{13}C_\beta$	−2674	−2147	−2.5
	$^{13}C_\alpha$–$^{13}C_{carboxyl}$	−2661	−2117	−2.61

total dephasing time τ_{total} of 551.72 μs. Experimental values of the effective dipolar couplings for the observed ^{13}C DQ spin-pairs are shown in comparison with the predicted values in Table 1. Experimental and predicted values agree reasonably well. The experiment could probably be improved either by using DQ no-decoupling pulse sequences [44,45] or by more efficient decoupling schemes [46]. The 2D DQ dephasing experiment might be interesting for applications in amorphous materials in terms of distance distribution functions.

5. Experimental section

The ^{13}C and ^{31}P NMR experiments were carried out on a Varian Infinity+ NMR spectrometer equipped with a commercial 2.5 mm double-resonance MAS-NMR probe. The magnetic field strength was 9.4 T corresponding to resonance frequencies of $\nu(^{31}P) = 161.4$ MHz and $\nu(^{13}C) = 100.9$ MHz. Samples were rotated within zirconia spinners. By means of appropriate spacers, the sample was confined to the middle 1/3 of the rotor volume. A commercially available pneumatic control unit was used to limit MAS frequency variations to a 2 Hz interval for the duration of the experiment. For crystalline $Ag_7P_3S_{11}$ the spinning frequency ν_r was set to 10 kHz and for alanine to 7250 Hz, respectively. During the PostC7 sequence this required pulse nutation frequencies of 70 and 50.75 kHz, respectively. A saturation comb was used to erase the phase memory of the spins, since for both samples the repetition times were too short with respect to spin–lattice relaxation times. The saturation comb was used in front of every scan and typically consisted of 10–20 pulses with a 90° flip-angle and a delay of typically 50 ms.

The numerical simulations of the spin-dynamics were done using the SIMPSON NMR interpreter published by Nielsen and co-workers [47]. Powder averages were chosen according to the Zaremba–Conroy–Wolfsberg scheme [48] with a number of orientations of 1760 (88 α-, β-angle-pairs × 20 γ-angles) or better. The integration time step for the DQ simulations was chosen as 1/10th of the shortest RF-unit in the sequence.

6. Conclusions

In this contribution a new pulse sequence (Double-Quantum Dephasing, DoDe) is described which is useful for the determination of homonuclear dipolar interaction of spin-1/2 nuclei. It is suitable both for diluted and dense multiple-spin systems and relies on the dephasing of double-quantum coherence. Normalization and relaxation problems can be minimized by the use of a constant-time sampling method of the dephasing curve. In multiple-spin systems the initial part of the DQ dephasing curve was shown to be sensitive to lattice sums of dipolar coupling constants.

For a single distance-determination DoDe requires only two experimental data points. Together with a 2D protocol it was shown that this feature can be used to measure a set of dipolar interactions from two separate 2D experiments. In terms of signal to noise DoDe experiments profit from the idea of dephasing which improves signal to noise ratios. At the same time the total number of experiments for a single distance is of the same order or even shorter than for ordinary DQ build-up techniques.

DoDe experiments will be useful in the characterization of amorphous samples because distributions of dipolar interactions can be extracted from 2D DoDe spectra. In this context the signal to noise ratio might further be improved by combing DoDe with the refocused INADEQUATE [31,49] experiment and if feasible cross-polarization. DoDe experiments are also ideally suited to help in the assignment of ^{31}P resonances in phosphates via the effective dipolar coupling constant.

Acknowledgments

Financial support by the Deutsche Forschungsgemeinschaft through the Emmy-Noether program is gratefully acknowledged. I am grateful to Malcolm H. Levitt for pointing me to the difficult case of weak couplings next to strong dipolar couplings, Kay Saalwächter for discussing

his normalization approach, Wilfried Hoffbauer for experimental support, Jürgen Senker for comments on the manuscript and Hellmut Eckert for many inspiring conversations.

Appendix A. Supplementary data

Supplementary data associated with this article can be found, in the online version, at doi:10.1016/j.jmr.2006.02.009.

References

[1] J.H. van Vleck, The dipolar broadening of magnetic resonance lines in crystals, Phys. Rev. 74 (1948) 1168–1183.
[2] G.R. Miller, H.S. Gutowsky, NMR study of the alkali hexafluorophosphates' dynamic structure, J. Chem. Phys. 39 (1963) 1983–1994.
[3] R. Goc, Simulation of the NMR second moment as a function of temperature in the presence of molecular motion. Application to $(CH_3)_3NBH_3$, Z. Naturforsch. 57a (2002) 29–35.
[4] M. Bertmer, H. Eckert, Dephasing of spin echoes by multiple heteronuclear dipolar interactions in rotational echo double resonance NMR experiments, Solid State Nucl. Magn. Reson. 15 (1999) 139–152.
[5] Y. Pan, T. Gullion, J. Schaefer, Determination of C–N internuclear distances by rotational-echo double resonance NMR of solids, J. Magn. Reson. 90 (1990) 330–340.
[6] X. Zhao, W. Hoffbauer, J. Schmedt auf der Günne, M.H. Levitt, Heteronuclear polarization transfer by symmetry-based recoupling sequences in solid-state NMR, Solid State Nucl. Magn. Reson. 26 (2004) 57–64.
[7] J.C.C. Chan, C-REDOR: rotational echo double resonance under very fast magic-angle spinning, Chem. Phys. Lett. 335 (2001) 289–297.
[8] S. Dusold, A. Sebald, Dipolar recoupling under magic-angle spinning conditions, Annu. Rep. NMR Spectrosc. 41 (2000) 185–264.
[9] S.P. Brown, H.W. Spiess, Advanced solid-state NMR methods for elucidation of structure and dynamics of molecular, macromolecular, and supramolecular systems, Chem. Rev. 101 (2001) 4125–4155.
[10] S. Hafner, D.E. Demco, Solid-state NMR spectroscopy under periodic modulation by fast magic-angle sample spinning and pulses: a review, Solid State Nucl. Magn. Reson. 22 (2002) 247–274.
[11] Y. Ishii, J.J. Balbach, R. Tycko, Measurement of dipole-coupled lineshapes in a many-spin system by constant-time two-dimensional solid state NMR with high-speed magic-angle spinning, Chem. Phys. 266 (2001) 231–236.
[12] M. Hohwy, C. Rienstry, R.G. Griffin, Band-selective homonuclear dipolar recoupling in rotating solids, J. Chem. Phys. 117 (2002) 4973–4987.
[13] K. Saalwächter, P. Ziegler, O. Spyckerelle, B. Haidar, A. Vidal, J.-U. Sommer, ^{1}H multiple-quantum nuclear magnetic resonance investigations of molecular order distributions in poly(dimethylsiloxane) networks: evidence for a linear mixing law in bimodal systems, J. Chem. Phys. 119 (2003) 3468–3482.
[14] A.E. Bennett, C.M. Rienstra, J.M. Griffiths, W. Zhen, P.T.J. Lansbury, R.G. Griffin, Homonuclear radio frequency-driven recoupling in rotating solids, J. Chem. Phys. 108 (1998) 9463–9479.
[15] L. Sonnenberg, S. Luca, M. Baldus, Multiple-spin analysis of chemical-shift-selective (^{13}C, ^{13}C) transfer in uniformly labeled biomolecules, J. Magn. Reson. 166 (2004) 100–110.
[16] R. Graf, D.E. Demco, J. Gottwald, S. Hafner, H.W. Spiess, Dipolar couplings and internuclear distances by double-quantum nuclear magnetic resonance, J. Chem. Phys. 106 (1997) 885–895.
[17] M. Feike, D.E. Demco, R. Graf, J. Gottwald, S. Hafner, H.W. Spiess, Broadband multiple-quantum NMR spectroscopy, J. Magn. Reson. A122 (1996) 214–221.
[18] Y.K. Lee, N.D. Kurur, M. Helmle, O.G. Johannessen, N.C. Nielsen, M.H. Levitt, Efficient dipolar recoupling in the NMR of rotating solids. A sevenfold symmetric radiofrequency pulse sequence, Chem. Phys. Lett. 242 (1995) 304–309.
[19] M. Hohwy, H.J. Jakobsen, M. Edén, M.H. Levitt, N.C. Nielsen, Broadband dipolar recoupling in the nuclear magnetic resonance of rotating solids: a compensated C7 pulse sequence, J. Chem. Phys. 108 (1998) 2686–2694.
[20] E. Diéz-Peña, I. Quijada-Garrido, J.M. Barrales-Rienda, I. Schnell, H.W. Spiess, Advanced ^{1}H solid-state NMR spectroscopy on hydrogels, 2[a] the formation of hydrogen bonds in hydrogels based on *N*-isopropylacrylamide (NiPAAm) and methacrylic acid (MAA), Macromol. Chem. Phys. 205 (2004) 438–447.
[21] A. Rapp, I. Schnell, D. Sebastiani, S.P. Brown, V. Percec, H.W. Spiess, Supramolecular assembly of dendritic polymers elucidated by ^{1}H and ^{13}C solid-state MAS NMR spectroscopy, J. Am. Chem. Soc. 125 (2003) 13284–13297.
[22] N. Hedin, R. Graf, S.C. Christiansen, C. Gervais, R.C. Hayward, J. Eckert, B.F. Chmelka, Structure of a surfactant-templated silicate framework in the absence of 3D crystallinity, J. Am. Chem. Soc. 126 (2004) 9425–9432.
[23] M.H. Levitt, Symmetry-based pulse sequence in magic-angle spinning solid-state NMR, Encyc. NMR 9 (2002) 165–196.
[24] P. Hodgkinson, L. Emsley, The accuracy of distance measurements in solid-state NMR, J. Magn. Reson. 139 (1999) 46–59.
[25] P. Hodgkinson, D. Sakellariou, L. Emsley, Simulation of extended periodic systems of nuclear spins, Chem. Phys. Lett. 326 (2000) 515–522.
[26] A. Brinkmann, M. Edén, M.H. Levitt, Synchronous helical pulse sequences in magic-angle spinning nuclear magnetic resonance: Double quantum recoupling of multiple-spin systems, J. Chem. Phys. 112 (2000) 8539–8554.
[27] C. Filip, S. Hafner, I. Schnell, D.E. Demco, H.W. Spiess, Solid state NMR spectra of dipolar-coupled multi-spin systems under fast magic angle spinning, J. Chem. Phys. 110 (1999) 423–440.
[28] B. Reif, C.P. Jaroniec, C. Rienstra, M. Hohwy, R.G. Griffin, ^{1}H–^{1}H MAS correlation spectroscopy and distance measurements in a deuterated peptide, J. Magn. Reson. 151 (2001) 320–327.
[29] B. Reif, B.J. van Rossum, F. Castellani, K. Rehbein, A. Diehl, H. Oschkinat, Characterization of ^{1}H–^{1}H distances in a uniformly ^{2}H, ^{15}N-labeled SH3 domain by MAS solid-state NMR spectroscopy, J. Am. Chem. Soc. 125 (2003) 1488–1489.
[30] M. Carravetta, M. Edén, O.G. Johannessen, H. Luthman, P.J.E. Verdegem, J. Lugtenburg, A. Sebald, M.H. Levitt, Estimation of carbon–carbon bond lengths and medium-range internuclear: distances by solid-state nuclear magnetic resonance, J. Am. Chem. Soc. 123 (2001) 10628–10638.
[31] A. Lesage, M. Bardet, L. Emsley, Through-bond carbon–carbon connectivities in disordered solids by NMR, J. Am. Chem. Soc. 121 (1999) 10987–10993.
[32] A. Bax, R. Freeman, S.P. Kempsell, Natural abundance ^{13}C–^{13}C coupling observed via double-quantum coherence, J. Am. Chem. Soc. 102 (1980) 4849–4851.
[33] J. Schmedt auf der Günne, J. Beck, W. Hoffbauer, P. Krieger-Beck, The structure of poly(carbonsuboxide) on the atomic scale—a solid-state NMR study, Chem. Eur. J. 11 (2005) 4429–4440.
[34] A.E. Bennett, D.P. Weliky, R. Tycko, Quantitative conformational measurements in solid state NMR by constant-time homonuclear dipolar recoupling, J. Am. Chem. Soc. 120 (1998) 4897–4898.
[35] J. Schmedt auf der Günne, Distance measurements in spin-1/2 systems by ^{13}C and ^{31}P solid-state NMR in dense dipolar networks, J. Magn. Reson. 165 (2003) 18–32.

[36] Y. Ishii, ^{13}C–^{13}C dipolar recoupling under very fast magic angle spinning in solid-state nuclear magnetic resonance: applications to distance measurements, spectral assignments, and high-throughput secondary-structure determination, J. Chem. Phys. 114 (2001) 8473–8483.
[37] M.H. Levitt, P.K. Madhu, C.E. Hughes, Cogwheel phase cycling, J. Magn. Reson. 155 (2002) 300–306.
[38] M. Carravetta, M. Edén, X. Zhao, A. Brinkmann, M.H. Levitt, Symmetry principles for the design of radiofrequency pulse sequences in the nuclear magnetic resonance of rotating solids, Chem. Phys. Lett. 321 (2000) 205–215.
[39] J.M. Goetz, J. Schaefer, REDOR dephasing by multiple spin in the presence of molecular motion, J. Magn. Reson. 127 (1997) 147–154.
[40] M. Hohwy, C.M. Rienstra, C.P. Jaroniec, R.G. Griffin, Fivefold symmetric homonuclear dipolar recoupling in rotating solids: application to double quantum spectroscopy, J. Chem. Phys. 110 (1999) 7983–7992.
[41] A.K. Roy, K.K. Gleason, Analytical solutions for multiple-quantum-coherence dynamics among two or three dipolar-coupled, spin 1/2 nuclei, J. Magn. Reson. A120 (1996) 139–147.
[42] C. Brinkmann, H. Eckert, D. Wilmer, M. Vogel, J. Schmedt auf der Günne, W. Hoffbauer, F. Rau, A. Pfitzner, Re-entrant phase transition of the crystalline ion conductor $Ag_7P_3S_{11}$, Solid State Sci. 6 (2004) 1077–1088.
[43] J.D. Gehman, E.K. Paulson, K.W. Zilm, The influence of internuclear spatial distribution and instrument noise on the precision of distances determined by solid state NMR of isotopically enriched proteins, J. Biomol. NMR 27 (2003) 235–259.
[44] C.E. Hughes, S. Luca, M. Baldus, Radio-frequency driven polarization transfer without heteronuclear decoupling in rotating solids, Chem. Phys. Lett. 385 (2004) 435–440.
[45] I. Marin-Montesinos, D.H. Brouwer, G. Antonioli, W.C. Lai, A. Brinkmann, M.H. Levitt, Heteronuclear decoupling interference during symmetry-based homonuclear recoupling in solid-state NMR, J. Magn. Reson. 177 (2005) 330–340.
[46] A. Detken, E.H. Hardy, M. Ernst, B.H. Meier, Simple and efficient decoupling in magic-angle spinning solid-state NMR: the XiX scheme, Chem. Phys. Lett. 356 (2002) 298–304.
[47] M. Bak, J.T. Rasmussen, N.C. Nielsen, SIMPSON: a general simulation program for solid-state NMR spectroscopy, J. Magn. Reson. 147 (2000) 296–330.
[48] H. Conroy, Molecular Schrödinger equation. VIII. A new method for the evaluation of multidimensional integrals, J. Chem. Phys. 47 (1967) 5307–5318.
[49] A. Lesage, C. Auger, S. Caldarelli, L. Emsley, Determination of through-bond carbon–carbon connectivities in solid-state NMR using the INADEQUATE experiment, J. Am. Chem. Soc. 119 (1997) 7867–7868.
[50] P. Toffoli, P. Khodadad, N. Rodier, Structure du tétrathiomonophosphate(V) Heptathiodiphosphate(V) d'Argent, Acta Crystallogr. B38 (1982) 2374–2378.
[51] M.S. Lehmann, T.F. Koetzle, W.C. Hamilton, Precision neutron diffraction structure determination of protein and nuclei acid components. I The crystal and molecular structure of amino acid L-alanine, J. Am. Chem. Soc. 94 (1972) 2657–2660.